Adaptive silver films towards bio-array applications

Vladimir P. Drachev*, Meena L. Narasimhan[1], Hsiao-Kuan Yuan, Mark D. Thoreson, Yong Xie[2], V. Jo Davisson[1], and Vladimir M. Shalaev
School of Electrical and Computer Engineering, [1]Bindley Bioscience Center, and [2]Department of Chemistry, Purdue University, West Lafayette, IN 47907

ABSTRACT

Adaptive silver films (ASFs) have been studied as a substrate for protein microarrays. Vacuum evaporated silver films fabricated at certain range of evaporation parameters allow fine rearrangement of the silver nanostructure under protein depositions in buffer solution. Proteins restructure and stabilize the ASF to increase the surface-enhanced Raman scattering (SERS) signal from a monolayer of molecules. Preliminary evidence indicates that the adaptive property of the substrates make them appropriate for protein microarray assays. Head-to-head comparisons with two commercial substrates have been performed. Protein binding was quantified on the microarray using the streptavidinCy3/biotinylated goat IgG protein pair. With fluorescence detection, the performance of ASF substrates was comparable with SuperAldehyde and SuperEpoxy substrates. Additionally, the ASF is also a SERS substrate and this provides an additional tool for analysis. It is found that the SERS spectra of the streptavidinCy5 fluorescence reporter bound to true and bound to false sites show distinct difference.

Keywords: protein microarray, metal nanostructures, SERS

1. INTRODUCTION

Detection of protein-ligand binding events most commonly involve labeling strategies with a variety of detection schemes including scintillation counting [1], electrochemical changes [2], enzymatic transformation [3], fluorescence [4,5], chemiluminescence [6], or quantum dots [13]. More recent advances involve the use of surface plasmon resonance (SPR) [7-9], or surface enhanced Raman scattering (SERS) [10-12]. One of the SERS-based approaches takes advantage of the binding properties of antibody and antigen molecules (or DNA strands) and uses metal nanoparticles coated with Raman-active chromophores as tags [15-17]. To provide the needed level of enhancement, silver clusters are added to form a complex sandwich structure that includes a nanoparticle labeled with a Raman active dye, complementary bio-molecules and the metal clusters. The detection of SERS events without inclusion of exogenous labels has been previously employed for an immune reaction using colloidal gold particles [18]. Other applications of SERS detection for binding to proteins include aflatoxins to RNA polymerase and specific organisms to their respective antibodies [19].

Adaptive silver films have recently been reported as SERS substrates that allow protein sensing at monolayer surface density [20]. The adaptive property of this substrate enabled adsorption of proteins without significant alteration in their conformational state. In an example using human insulin and insulin lispro, the results showed that the SERS spectra reveal unique features attributable to distinct conformational states, which was in agreement with X-ray crystallographic studies [20].

Direct, label-free detection of antibody-antigen binding at a monolayer protein concentration has been also demonstrated, using SERS detection on adaptive silver films [21]. This includes evidence of distinct SERS spectral changes upon antigen-antibody binding as well as independent immunochemical assay validation which confirms that the antibodies retain binding properties on ASFs. An additional increase in the SERS enhancement by factor of 4-5 has been demonstrated in [22] with a multilayer ASF containing an additional thick mirror-like Ag sublayer.
We show here that the adaptive property of the evaporated silver film substrates has potential for protein microarray applications. In a preliminary comparison of the binding reaction of streptavidin-Cy3 with biotinylated goat IgG on

* vdrachev@ecn.purdue.edu, phone 1 765 494-0628; fax 1 765 494-6951

ASF substrates and two commercial microarray substrates using fluorescence detection, the performance of ASF substrates was comparable with the commercial microarray substrates. Additionally, the SERS spectra of streptavidinCy5 fluorescence reporter showed distinct differences between specific and false site binding events.

2. MATERIALS AND METHODS

2.1 Preparation of Adaptive Silver Films

Fabrication of a nanostructured ASF involves deposition of films on a dielectric substrate under vacuum evaporation with an electron beam. Microscope glass slides (Fisher Scientific, Hanover Park, IL, USA) were cut into 2.5 cm x 2.5 cm sections for use as initial substrates. The cut slides were cleaned through several steps, including triple rinses in acetone and methanol solvents, a piranha (H_2O_2:$3H_2SO_4$) acid bath, rinsing in 18 MΩ deionized water, and drying with pressurized gaseous nitrogen. Silver shot (99.9999 %, 1-3 mm; Alfa Aesar, Ward Hill, MA, USA) and SiO_2 pellets (99.995 %; Kurt J. Lesker, Pittsburgh, PA, USA) were used for fabrication of the ASFs on the cleaned glass slides. The thin film deposition was performed in a modified Varian electron-beam evaporator with an initial pressure inside the system of approximately 10-7 Torr. The film thickness and deposition rate were monitored with a quartz crystal oscillator. The glass slides were covered first by a sublayer of SiO_2 (10 nm) followed by a silver layer (10-13 nm) deposited at a rate of 0.05 nm/s. The fabricated films were characterized by field emission scanning electron microscopy (FE SEM), atomic force microscopy (AFM), and a Lambda 35 spectrophotometer (Perkin-Elmer, Boston, MA, USA) equipped with a Labsphere. High-resolution FE SEM images were obtained through MAS, Inc. (Raleigh, NC, USA). AFM images (not shown here) were acquired with a Dimension 3100 (DI Veeco) using a 10 nm Si tip for measuring the height profiles.

2.2 Materials

Cy5- and Cy3-labelled streptavidin were obtained from Amersham Biosciences (Piscataway, NJ, USA). Anti-rabbit immunoglobulin G (IgG) developed in goat was obtained as a biotin conjugate from Stressgen (Victoria, BC, Canada). Anti-human interleukin 6 monoclonal antibody (mouse IgG1) was obtained as a preservative- and carrier-free formulation in PBS (Pierce Biotechnology, Rockford, IL, USA or Endogen, Woburn, MA, USA). Tris buffered saline (TBS) with composition: 50 mM Tris.HCl pH 8.0, 0.138 M NaCl, 2.7 mM KCl , BSA (Fraction V), and Tween 20 were obtained from Sigma (St. Louis, MO, USA). Phosphate buffered saline (PBS) was purchased from Pierce Biotechnology. ArrayIt Super Aldehyde and Super Epoxy Substrates were obtained from Tele-Chem International (Sunnyvale, CA, USA). Water (HPLC grade) used in these studies was obtained from Burdick and Jackson (Muskegon, MI, USA).

2.3 Protein Microarray Assay

The capture proteins (IgGs) were dissolved in PBS buffer (300 μg/mL) for spotting on the ASF substrate. They were dissolved in ArrayIt Protein Printing buffer (300 μg/mL) for printing on ArrayIt Super Epoxy and ArrayIt Super Aldehyde substrates. The approximate spotting volume was 0.7 nL, yielding spots of about 100 μm in diameter. All slides were custom printed by Tele-Chem International. The slides were stored in a dark chamber at room temperature until use. Printed slides were washed for 20 min in TBS with gentle agitation and blocked with milk (3% w/v) or BSA (3% w/v) in TBS for 30 min. For quantification assays, the slides were incubated for 2.5 h with Cy3-labeled streptavidin diluted in TBS containing 3% w/v BSA. For sandwich immunoreactions, the arrays were blocked with milk and incubated for 3 h with human interleukin 6 (IL-6; 4.6 pg/mL) in TBS containing 0.1% w/v BSA; 0.02% w/v Tween 20 and washed with TBS containing 0.1% Tween 20 before a 1h incubation with biotinylated secondary antibody (1:10 dilution; FAST Quant kit; Schleicher and Schuell, Keene, NH) dissolved in TBS. The slides were then washed with TBS containing 0.1% Tween 20 and incubated for 1h with Cy5-linked streptavidin (0.125 μg/ml) in TBS. After reaction with the fluor-linked reagent, the slides were washed successively with TBS containing 0.1% Tween 20 and TBS, rinsed with water, dried using canned air and scanned for fluorescence evaluation.

2.4 Scanning and evaluation

All fluorescence signals were detected with a ScanArray 4000 unit (Packard Biosciences, Billerica, MA, USA) using the same photomultiplier tube (PMT) gain and laser power for all of the slides. Images were analyzed with the ImageQuant software package (Amersham Biosciences). Data were exported to Microsoft Excel software for further processing and statistical analyses. Signal intensities were expressed in arbitrary units.

2.5 Acquisition of SERS Spectra

Spectra were collected at a laser wavelength of 568 nm, 1 mW power, an exposure time of 200 s and were subjected to background subtraction using a Fourier method. A four-wavelength Raman system was used that consisting of an Ar/Kr

ion laser (Melles Griot), a laser band-path holographic filter (to reject plasma lines), two Super-Notch Plus filters to reject Rayleigh scattering (Kaiser Optical Systems), focusing and collection lenses, an Acton Research 300i monochromator with a grating of 1200 grooves/mm, and a nitrogen-cooled CCD (1340 x 400 pixels, Roper Scientific). An objective lens (f/1.6) provided a collection area of about 180 μm^2. Collected light was delivered to the monochromator via a fiber bundle. The spectral resolution was about 3 cm^{-1} with the laser power approximately 1 mW and exposure time of 100-200 s.

3. RESULTS AND DISCUSSION

3.1 Adaptive Silver Films

Metal films have been used for SERS studies for many years [17, 22-25]. Their physical and optical properties depend on evaporation parameters, mass thickness, and the material in the sub-layer(s). In our recent work, silver films fabricated at a certain range of evaporation parameters allow fine rearrangement of the nanostructure upon protein deposition [20]. This restructuring forms cavity sites enclosed by two or more particles, which have optimal spacing for SERS. In this case, these cavity sites are naturally filled with the protein molecules. Because of these features, a nanostructured evaporated film that allows restructuring is herein referred to as *adaptive*. Previous experiments with ASFs show that SERS spectral differences attributed to the distinct conformational states of human insulin and its analog, insulin lispro, can be observed at sub-monolayer protein molecule coverage [20]. The measured macroscopic enhancement factor is about $3x10^6$, which is among the largest observed for random metal-dielectric films.

Fig. 1: Spot of anti-interleukin 10 on an ASF after deposition of 2 μL at concentration a) 0.5 μM and b) 2 μM

Fig. 1 shows two typical protein spots (before washing with buffer) deposited in TBS buffer on an ASF. In the example in the figure, the concentration of the deposited antibody was 0.5 μM (left) and 2 μM (right). The protein spot is surrounded by a transparent area resulting from the spread of buffer during drying. At higher concentration, part of the protein solution forms a ring outside the central spot after drying, indicating that the protein concentration is above optimal. After washing with TBS/Tween-20, the non-adherent metal is removed from the substrate except in the areas where protein (antibody or antigen) has been deposited (not shown).

The nanostructure of the ASF before and after protein deposition and washing are shown in Figure 2. As illustrated by the FE SEM images (Fig. 2b, c), the protein-mediated restructuring results in the formation of aggregates of silver particles covered with proteins (Fig. 2b, c), as opposed to the relatively disintegrated albeit closely-spaced particles of the initial film before protein deposition (Fig. 2a). Depending on the mass thickness of the initial film, small or large fractal-like aggregates can be formed. The small aggregates are not shown here, but are similar to those shown in [20] for insulin.

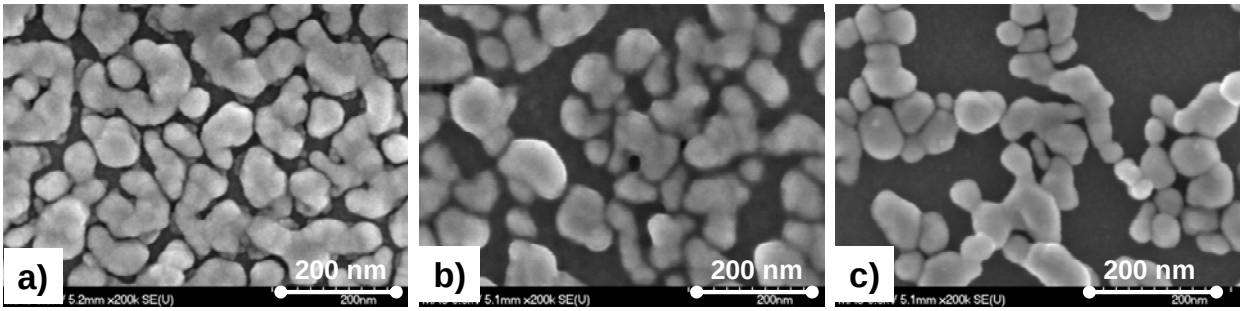

Fig. 2: FE SEM images of two substrates from one batch: a) 12 nm silver film (transmission at 568 nm T= 0.27); b) 12 nm silver film inside antibody spot (T= 0.23-0.27); c) same substrate as b) but inside antigen (bacterial alkaline phosphatase tagged with FLAG polypeptide at C-terminal) spot (T=0.4). Images collected 8 weeks after fabrication; proteins deposited one week after fabrication.

A lower concentration of protein results in lower metal coverage (the ratio of white area to total area in the FE SEM images). Fig. 2b and c show that a decrease of metal coverage correlates with the decreasing optical absorption (transmission T= 0.25 for 2b and T=0.4 for 2c). The absorbance of the metal film inside a protein spot increases linearly with protein concentration and then saturates above a certain concentration which can be considered as optimal (Fig. 3). The concentration dependence shows almost no change after 30 min of washing in TBS/Tween 20 solution (the circles in Fig. 3), which confirms the stabilization of the film by the proteins.

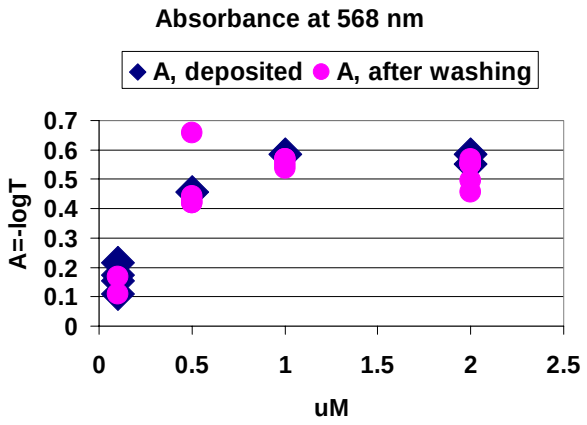

Fig. 3: Absorbance inside protein spot (anti-interleukin 10) versus protein concentration.

The transparent areas outside of a typical protein spot certainly contain no silver particles as it follows from absorption measurements. The metal particle coverage inside the protein spot is also reduced relative to the initial film. To determine the chemical form of the silver remaining in the transparent areas, TBS (Tris(Hydroxymethyl)aminomethane(NH_2-C-(CH_2OH)$_3$): 0.05 M ; NaCl: 0.138 M; KCl: 0.0027 M -> [Cl^-]: 0.1407 M) was deposited on the ASF and dried. Then the deposition region was studied with FE SEM and X-ray diffraction analysis. The transparent area contains 40x40 µm square particles as seen from FE SEM images (not shown). X-ray diffraction results shown in Fig. 4 indicate a reduced Ag 101 peak and two peaks from NaCl and AgCl. This implies that silver particles are transformed to silver salt in the transparent area. Typically, the AgCl peak is masked by the neighboring NaCl peak, which has a higher intensity. The presence of AgCl crystals can be seen more clearly in the X-ray diffraction spectra of an ASF treated with TBS after 10 s washing in water (not shown) and in the X-ray diffraction angular spectrum of an ASF treated with 1mM HCl (Fig. 4).

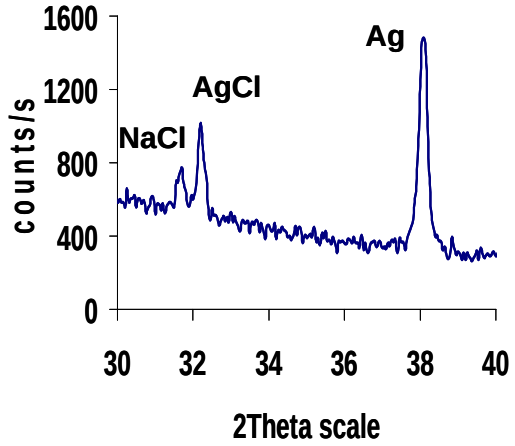

Fig. 4: X-ray diffraction of an ASF treated with 1mM HCl without proteins (transparent area).

An estimate of thermodynamics of the (redox) reaction of Ag with oxygen shows that Ag oxidation is a downhill reaction (with negative free energy) under our experimental conditions. When the silver film is exposed to a TBS buffer (pH 7.4), metal silver tends to be oxidized by oxygen and form AgCl. Due to the low solubility of AgCl in water (K_{sp}=1.8x10^{-10}) [27], the reduction reaction and its standard reduction potential of silver are:

$Ag+Cl^- = AgCl + e^-$, $E_{red}° = 0.2223$ V [27]

The oxidation reaction of oxygen in air can be expressed as:

$O_2+H^++4e^-=H_2O$, $E_{ox}° = 1.229$ V [27]

Therefore, the total reaction and its standard potential under standard condition [27] will be:

$4Ag+4Cl^-+O_2+4H^+=4AgCl+2H_2O$, $E°= E_{ox}°- E_{red}° = 1.007$ V

For calculating the actual reaction potential under the experimental condition at 298 K, we need to use the Nernst equation:

$E=E°- (0.059/4)\log\{1/([Cl^-]^4\ [H^+]^4\ P_{O2}\}$

From the experimental condition we know the concentration of chloride ion is about 0.1407 M, $[H^+]$ is about $10^{-7.4}$ M and the partial pressure of oxygen in air is 0.21 atm. So the experimental value of E is estimated to be 0.51 V which means that the reaction is thermodynamically favorable (downhill in free energy). The positive potential is the driving force for the oxidation of Ag to Ag^+.

3.2 SERS difference spectra for fluorescent reporter -streptavidinCy5

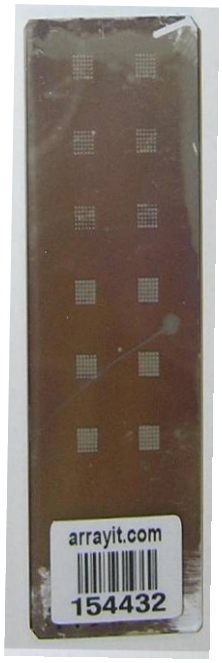

Fig.5 Antibody array on an ASF substrate

Figure 5 shows two 6 x 6 protein arrays deposited on an ASF substrate for the fluorescence detection experiment. Following the standard procedure described in Methods, the arrays containing deposits of anti-human IL-6 were blocked with milk. The arrays were then separated with spacers (FAST frame, Schleicher and Schuell), and the upper array was reacted with human IL-6 whereas the lower array was reacted with buffer lacking human IL-6. After reaction, both arrays were treated identically with biotinylated secondary antibody and then with Cy5-conjugated streptavidin. SERS

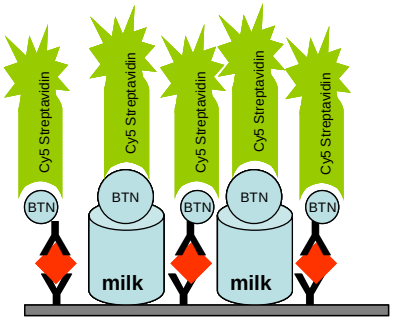

Fig. 6: Antibody-Antigen-biotinylated secondary Antibody-StreptavidinCy5 sandwich for fluorescence detection. Nonspecific binding to biotin in milk is also shown.

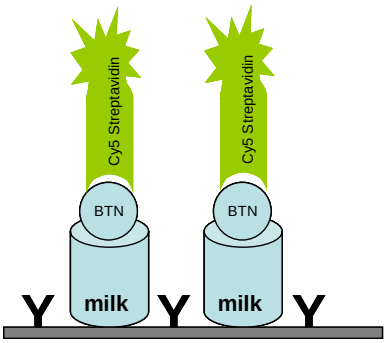

Fig. 7: Array squares for negative control. No antigen, only nonspecific binding.

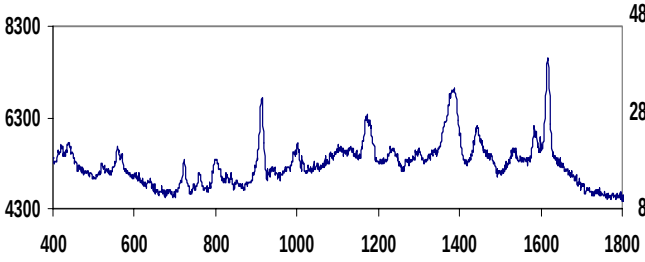

Fig. 8: SERS spectrum of streptavidinCy5 bound to the sandwich (related to Fig. 6)

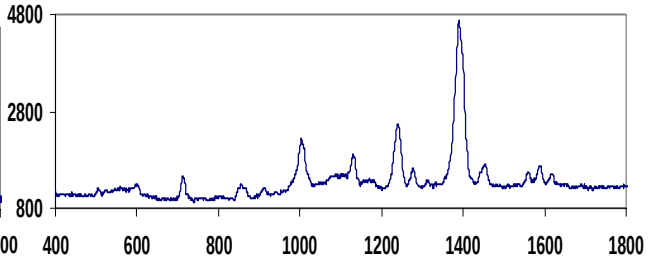

Fig. 9: SERS spectrum of streptavidinCy5 collected from the negative control squares (false sites).

spectra were acquired from the spots containing anti human IL-6 in both arrays. Fluorescence images of the array showed signal from both arrays in islands containing anti-human IL-6. The fluorescence intensity was higher for the array that had been exposed to the cognate antigen (human IL-6). The signal from the negative control squares (not exposed to human IL-6) was faint but clearly detectable, probably due to the presence of biotin molecules in the blocker (milk) that provide undesirable binding sites for streptavidinCy5. It is impossible to distinguish these false sites from specific sites with fluorescence detection. Our results with SERS detection of the same array reveal strongly different spectra for the specific and false sites as is shown in Figs. 8 and 9 (spectra are presented "as is" *without* background subtraction). Since the interaction of biotin with streptavidin forms the basis of several widely used detection methods in bio-array technology, this application of the SERS detection could be very important.

3.3 Head-to-head comparison between ASF and commercial protein microarray substrates with fluorescence detection

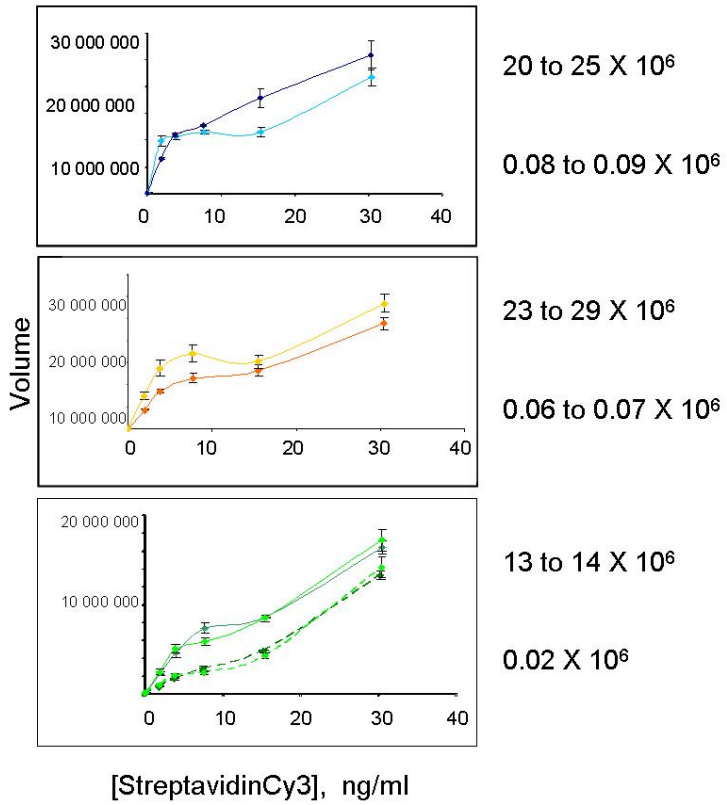

Fig. 10: Fluorescence signal vs concentration for ASF (top), SuperAldehyde (middle), and Superepoxy (bottom) substrates.

A head-to-head comparison of ASF substrates with commercially-available SuperAldehyde and SuperEpoxy substrates in microarray applications was initiated because the protein attachment process is known to influence the performance of protein microarray surfaces [28]. As before (Fig. 5), the arrays consisted of 36 spots arrayed in a 6 x 6 pattern. Twelve such arrays containing biotinylated anti-rabbit IgG were printed on each microscope slide so that each array could be separated using the FAST frame and treated under a different reaction condition. As indicated in Methods, the arrays were blocked with BSA and then reacted with the indicated concentrations of streptavidinCy3 (Fig. 10). The results of fluorescence imaging and analysis are shown in Fig. 10. The maximum average signal and background signal are shown at the right side of the graphs. Signal intensities on the ASF substrate were higher than those on the SuperEpoxy slides and comparable to the SuperAldehyde slides. However, the SuperEpoxy substrate (recommended for proteins) outperformed the other two substrates for low background and low spot-to-spot variation. Namely, the signal to background ratio is about 300 for ASF, 400 for SuperAldehyde, and 700 for SuperEpoxy substrates. The data show that the ASF substrates have potential for development as protein microarray surfaces for fluorescence applications.

4. CONCLUSIONS

Protein-mediated restructuring of silver films is always accompanied by a decrease in both the number of silver particles on the surface and film absorbance. Deposition of protein at low concentration in buffer results in chemical transformation of Ag from metal particles to AgCl crystals as suggested by our X-ray diffraction, absorbance, and FE SEM data. ASF substrates used for protein microarrays reveal a promising opportunity to detect SERS spectra along

with a fluorescence signal. Results from a microarray prepared using a quill-type spotter show that ASF substrates enable both fluorescence (with excitation at 633 nm) and SERS with no fluorescence (excitation at 568 nm) for the streptavidinCy5 fluorescence reporter. SERS spectra of streptavidinCy5 can be used to distinguish between desirable and undesirable binding events. With fluorescence detection, the performance of ASF was comparable with two commercial substrates. More detail results and analysis will be published elsewhere.

ACKNOWLEDGEMENTS

We thank Dr. Ben-Amotz and V. Nashine for fruitful discussions. This work was supported by Inproteo.

REFERENCES

1. S. Gutcho, L. Mansbach, *Clin. Chem.* 23, 1609 (1977).
2. F. J. Hayes, H. B. Halsall, and W. R. Heineman, *Anal. Chem.* 66, 1860 (1994).
3. J. E. Butler, *J. Immunoassay* 21, 165 (2000).
4. J. Vuori, S. Rasi, T. Takala, and K. Vaananen, *Clin. Chem.* 37, 2087 (1991).
5. Y. Y. Xu, K. Pettersson, K. Blomberg, I. Hemmila, H. Mikola, and T. Lovgren, *Clin. Chem.* 38, 2038 (1992).
6. C. R. Brown, K. W. Higgins, K. Frazer, L. K. Schoelz, J. W. Dyminski, V. A. Marinkovich, S. P. Miller, and J. F. Burd, *Clin. Chem.* 31, 1500 (1985).
7. L. A. Lyon, M. D. Musik, and M. J. Natan, *J. Anal. Chem.* 70, 5177 (1998).
8. W. Knoll, M. Zizlsperger, T. Liebermann, S. Arnold, A. Badia, M. Liley, D. Piscevic, F. J. Schmitt, and J. Spinke, *J. Colloid. Surf A* 161, 115 (2000).
9. B. P. Nelson, T. E. Grimsrud, M. R. Liles, R. M. Goodman, and R. M. Corn, *Anal. Chem.* 73, 1 (2001).
10. T. E. Rorh, T. Cotton, N. Fan, and P. J. Tarcha, *J. Anal. Biochem.* 182, 388 (1989).
11. X. Dou, T Takama, Y. Yamaguchi, H. Yamamoto, and Y Ozaki, *Anal. Chem.* 69, 1492 (1997).
12. J. Ni, R. J. Lipert, G. B. Dawson, and M. D. Porter, *Anal. Chem.* 71, 4903 (1999).
13. W. C. W. Chan and S. Nie, *Science* 281, 2016 (1998).
14. J. C. Riboh, A. J. Haes, A. D MacFarland, C. R. Yonzon, and R. P. Van Duyne, *J. Phys. Chem. B* 107, 1772 (2003).
15. Y. W. C. Cao, R. Jin, C. A. Mirkin, *Science* 297, 1536 (2002).
16. Y. C. Cao, R. Jin, C. S. Thaxton, and C. A. Mirkin, *J. Am. Chem. Soc.* 125, 14676 (2003).
17. T. Vo-Dinh and D. L. Stokes, pp. 64.1-64.39, in *Biomedical Photonics Handbook,* ed. by T. Vo-Dinh, CRC press LLC, Boca Raton (2003).
18. X. Dou, Y. Yamguchi, H. Yamamoto, S. Doi and Y. Ozaki, *J. Raman Spec.* 29, 739 (1998).
19. A. E. Grow, L. L. Wood, J. L. Claycomb, and P. A. Thomson, *J. Microbio. Methods* 53, 221 (2003).
20. V. P. Drachev, M. D. Thoreson, E. N. Khaliullin, V. J. Davisson, and V. M. Shalaev, *J. Phys. Chem. B* 108, 18046-18052 (2004).
21. V. P. Drachev, V. C. Nashine, M. D. Thoreson, D. Ben-Amotz, V. J. Davisson, and V. M. Shalaev, *Langmuir*, submitted.
22. V. P. Drachev, M. D. Thoreson, V. C. Nashine, E. N. Khaliullin, D. Ben-Amotz V. J. Davisson, and V. M. Shalaev, *J. Raman Spec.*, to be published.
23. C. Y. Chen, E. Burstein, and S. Lundqvist, *Solid State Commun.* 32, 63 (1979).
24. I. Pockrand and A. Otto, *Solid State Commun*. 35, 861 (1980)
25. J. G. Bergman, D. S. Chemla, P. F. Liao, A. M. Glass, A. Pinczuk, R. M. Hart, and D. H. Olson, *Opt. Lett.* 6, 33 (1981).
26. D. A. Weitz, S. Garoff, and T. J. Gramila, *Opt. Lett.* 7, 168 (1982).
27. Allen J. Bard, Roger Parsons, Joseph Jordan, Standard Potentials in Aqueous Solution, Publisher: Marcel Dekker, Inc., New York, 1985.
28. W. Kusnezow, J.D. Hoheisel, *J. Mol. Recognit.* 16, 165 (2003).